to environmental changes. Similarly to the control of diurnal and nocturnal activity by the mammalian SCN, understanding these interactions will require the characterization of the outputs of the clock neuron network. □

Methods

Fly strains

The *UAS-per16* insertion has been described previously[13]. *pdf-Gal4* is specifically expressed in both s-LN_vs and l-LN_vs[12], whereas *cry-Gal4-39* is expressed in the six clock neuronal groups of the adult brain: all LN_vs and LN_ds, most of the DN1 cells, the two DN2 cells and a fraction of the DN3 cells, in addition to several other neuronal groups that do not express clock genes[16]. Expression of the *C929-Gal4* enhancer trap has been described in about 100 peptidergic neurons of the adult brain, including the l-LN_vs, but not the s-LN_vs[17]. *Mai179-Gal4* enhancer trap expression has been reported in the PDF neurons of the larval brain[18], which become the s-LN_vs of the adult brain (see ref. 8). The *Mz520-Gal4* enhancer trap[20] is expressed in the PDF neurons of the adult brain (H. Otsuna and K. Ito, personal communication). See Fig. 2 for the characterization of *Mai179-Gal4* and *Mz520-Gal4* expression in the adult brain.

Behavioural analysis

Experiments were carried out with 1–7-day-old males at 20 °C in *Drosophila* activity monitors (TriKinetics) as previously described[13,21]. For DD analysis, flies were first entrained in 12/12 h LD cycles during 2–4 days, data were analysed for 6 days from the second day in DD. Data analysis was done with the Faas software 0.7.1, which is derived from the Brandeis Rhythm Package, and is available on request. Rhythmic flies were defined by χ^2 periodogram analysis with the following criteria (filter on): power $\geq$20, width $\geq$2 h, with no selection on period value. Power and width are the height and width of the periodogram peak, respectively, and give the significance of the calculated period. Mean daily activity (number of events per 0.5 h) is calculated over the whole period in LD or DD conditions. Waveforms: individual fly waveforms were calculated from the 6 days of analysis and normalized to 24 h; group waveforms were then calculated by averaging those individual waveforms. All behavioural experiments were reproduced two or three times with very similar results.

Immunolabellings

All experiments were done on whole-mounted adult brains (only males for PER; unsorted males and females for PDF and GFP labellings). GFP reporter expression, anti-PER and anti-PDF labellings were done as previously described[13,16,22]. Fluorescence signals were analysed with a Zeiss Axioplan2 epifluorescence microscope equipped with a SPOT2 (Diagnostic instruments) digital camera. Fluorescence intensity was quantified from digital images with the Adobe photoshop software. We applied the formula: $I = 100(S - B)/B$, which gives the fluorescence percentage above background (where S is fluorescence intensity and B is average intensity of the region adjacent to the positive cell).

Received 11 July; accepted 12 August 2004; doi:10.1038/nature02935.

1. Hall, J. C. Genetics and molecular biology of rhythms in *Drosophila* and other insects. *Adv. Genet.* **48,** 1–280 (2003).
2. Helfrich-Förster, C. Differential control of morning and evening components in the activity rhythm of *Drosophila melanogaster*—sex-specific differences suggest a different quality of activity. *J. Biol. Rhythms* **15,** 135–154 (2000).
3. Dunlap, J., Loros, J. & DeCoursey, P. J. (eds) *Chronobiology. Biological Timekeeping* (Sinauer Associates, Sunderland, Massachusetts, 2004).
4. Pittendrigh, C. & Daan, S. A Functional analysis of circadian pacemakers in nocturnal rodents. V. Pacemaker structure: a clock for all seasons. *J. Comp. Physiol. A* **106,** 333–335 (1976).
5. de la Iglesia, H. O., Meyer, J., Carpino, A. & Schwartz, W. J. Antiphase oscillation of the left and right suprachiasmatic nuclei. *Science* **290,** 799–801 (2000).
6. Yoshii, T. *et al. Drosophila* cry(b) mutation reveals two circadian clocks that drive locomotor rhythm and have different responsiveness to light. *J. Insect Physiol.* **50,** 479–488 (2004).
7. Jagota, A., de la Iglesia, H. O. & Schwartz, W. J. Morning and evening circadian oscillations in the suprachiasmatic nucleus *in vitro*. *Nature Neurosci.* **3,** 372–376 (2000).
8. Kaneko, M. & Hall, J. C. Neuroanatomy of cells expressing clock genes in *Drosophila*: transgenic manipulation of the period and timeless genes to mark the perikarya of circadian pacemaker neurons and their projections. *J. Comp. Neurol.* **422,** 66–94 (2000).
9. Frisch, B., Hardin, P. E., Hamblen-Coyle, M. J., Rosbash, M. & Hall, J. C. A promoterless period gene mediates behavioral rhythmicity and cyclical per expression in a restricted subset of the *Drosophila* nervous system. *Neuron* **12,** 555–570 (1994).
10. Kaneko, M., Park, J. H., Cheng, Y., Hardin, P. E. & Hall, J. C. Disruption of synaptic transmission or clock-gene-product oscillations in circadian pacemaker cells of *Drosophila* cause abnormal behavioral rhythms. *J. Neurobiol.* **43,** 207–233 (2000).
11. Helfrich-Förster, C. The period clock gene is expressed in central nervous system neurons which also produce a neuropeptide that reveals the projections of circadian pacemaker cells within the brain of *Drosophila melanogaster*. *Proc. Natl Acad. Sci. USA* **92,** 612–616 (1995).
12. Renn, S. C., Park, J. H., Rosbash, M., Hall, J. C. & Taghert, P. H. A pdf neuropeptide gene mutation and ablation of PDF neurons each cause severe abnormalities of behavioral circadian rhythms in *Drosophila*. *Cell* **99,** 791–802 (1999).
13. Blanchardon, E. *et al.* Defining the role of *Drosophila* lateral neurons in the control of circadian activity and eclosion rhythms by targeted genetic ablation and PERIOD protein overexpression. *Eur. J. Neurosci.* **13,** 871–888 (2001).
14. Cheng, Y. Z. & Hardin, P. E. *Drosophila* photoreceptors contain an autonomous circadian oscillator that can function without period mRNA cycling. *J. Neurosci.* **18,** 741–750 (1998).
15. Yang, Z. & Sehgal, A. Role of molecular oscillations in generating behavioral rhythms in *Drosophila*. *Neuron* **29,** 453–467 (2001).
16. Klarsfeld, A. *et al.* Novel features of cryptochrome-mediated photoreception in the brain circadian clock of *Drosophila*. *J. Neurosci.* **24,** 1468–1477 (2004).
17. Taghert, P. H. *et al.* Multiple amidated neuropeptides are required for normal circadian locomotor rhythms in *Drosophila*. *J. Neurosci.* **21,** 6673–6686 (2001).
18. Siegmund, T. & Korge, G. Innervation of the ring gland of *Drosophila melanogaster*. *J. Comp. Neurol.* **431,** 481–491 (2001).
19. Stoleru, D., Peng, P., Agosto, J. & Rosbash, M. Coupled oscillators control morning and evening locomotor behaviour of *Drosophila*. *Nature* doi:10.1038/nature02926 (this issue).
20. Ito, K., Urban, J. & Technau, G. Distribution, classification, and development of *Drosophila* glial cells in the late embryonic and early larval ventral nerve cord. *Roux Arch. Dev. Biol.* **204,** 284–307 (1995).
21. Klarsfeld, A., Leloup, J. C. & Rouyer, F. Circadian rhythms of locomotor activity in *Drosophila*. *Behav. Processes* **64,** 161–175 (2003).
22. Malpel, S., Klarsfeld, A. & Rouyer, F. Larval optic nerve and adult extra-retinal photoreceptors sequentially associate with the clock neurons during *Drosophila* brain development. *Development* **129,** 1443–1453 (2002).

Supplementary Information accompanies the paper on **www.nature.com/nature**.

Acknowledgements This work was supported by ACI 'Biologie du développement et physiologie intégrative' from the Ministère de la Recherche. F.R. is supported by INSERM, and R.X. is supported by Fondation des Treilles and previously by CNRS and Fondation Electricité de France. We thank M. Boudinot for the continuously improving Faas software, L. Collet for artwork, A. Klarsfeld and A. Lamouroux for critical reading of the manuscript, and J. Champagnat for his support. We thank J. Hall, P. Taghert and T. Siegmund for providing *pdf-Gal4, C929-Gal4* and *Mai179-Gal4* lines, respectively, as well as R. Stanewsky for anti-PER serum. We are grateful to H. Otsuna and K. Ito for sharing unpublished observations with the *Mz520-Gal4* line, and to M. Rosbash and colleagues for communicating their unpublished manuscript.

Competing interests statement The authors declare that they have no competing financial interests.

Correspondence and requests for materials should be addressed to F.R. (rouyer@iaf.cnrs-gif.fr).

Role of histone H2A ubiquitination in Polycomb silencing

Hengbin Wang[1], Liangjun Wang[2], Hediye Erdjument-Bromage[3], Miguel Vidal[4], Paul Tempst[3], Richard S. Jones[2] & Yi Zhang[1]

[1]*Department of Biochemistry and Biophysics, Lineberger Comprehensive Cancer Center, University of North Carolina at Chapel Hill, Chapel Hill, North Carolina 27599-7295, USA*
[2]*Department of Biological Sciences, Southern Methodist University, Dallas, Texas 75275, USA*
[3]*Molecular Biology Program, Memorial Sloan Kettering Cancer Center, 1275 York Avenue, New York, New York 10021, USA*
[4]*Departmamento de Desarrollo y Biologia Celular, Centro de Investigaciones Biologicas, Ramiro de Maeztu, 9, E28040 Madrid, Spain*

Covalent modification of histones is important in regulating chromatin dynamics and transcription[1,2]. One example of such modification is ubiquitination, which mainly occurs on histones H2A and H2B[3]. Although recent studies have uncovered the enzymes involved in histone H2B ubiquitination[4–6] and a 'cross-talk' between H2B ubiquitination and histone methylation[7,8], the responsible enzymes and the functions of H2A ubiquitination are unknown. Here we report the purification and functional characterization of an E3 ubiquitin ligase complex that is specific for histone H2A. The complex, termed hPRC1L (human Polycomb repressive complex 1-like), is composed of several Polycomb-group proteins including Ring1, Ring2, Bmi1 and HPH2. hPRC1L monoubiquitinates nucleosomal histone H2A at lysine 119. Reducing the expression of Ring2 results in a dramatic decrease in the level of ubiquitinated H2A in HeLa cells. Chromatin immunoprecipitation analysis demonstrated colocalization of dRing with ubiquitinated H2A at the PRE and

promoter regions of the *Drosophila Ubx* gene in wing imaginal discs. Removal of dRing in SL2 tissue culture cells by RNA interference resulted in loss of H2A ubiquitination concomitant with derepression of *Ubx*. Thus, our studies identify the H2A ubiquitin ligase, and link H2A ubiquitination to Polycomb silencing.

In order to identify the E3 ligase responsible for H2A ubiquitination, we developed an assay that allows us to monitor the enzyme activity. In the presence of E1, E2, ATP and Flag-ubiquitin (F-Ub), HeLa nuclear protein fractions were tested for E3 ligase activity with core histone octamer or nucleosomal histone substrates. Western blot analysis of the reactions using an antibody against Flag revealed a positive signal around 25 kDa, the size of H2A plus F-Ub, indicating that a potential H2A E3 ligase activity is present in the corresponding fractions (lanes 19–21 of the rectangular area in Fig. 1a). The activity is nucleosomal histone specific as parallel experiments using core histone octamers failed to detect such an activity (Fig. 1a, lanes 8–10). A weak activity potentially for H2B was also detected (Fig. 1a, lane 20). Since the 0.5 M P11 fraction derived from nuclear pellet has the strongest activity, we thus focused our further analysis on this fraction.

To verify that we have a real E3 ligase activity in the 0.5 M P11 fraction, we tested the dependence of the activity on each of the components in the reaction. Results shown in Fig. 1b indicate that the appearance of the ubiquitinated protein bands around 25 kDa depends on each component. To ascertain that the 25 kDa protein band is ubiquitinated H2A (uH2A), the protein band was subjected to mass spectrometry analysis which identified the protein as uH2A (Fig. 1c). Importantly, a peptide corresponding to the carboxy-terminal ubiquitin attached to Lys 119 of H2A was also identified. In addition, an antibody against uH2A recognizes the protein band specifically (data not shown). Thus, we conclude that we have identified an E3 ligase activity that specifically ubiquitinates H2A at Lys 119, a known *in vivo* ubiquitination site[9].

We monitored the enzymatic activity through seven chromatography columns (Fig. 2a) in order to identify the protein(s) responsible for the H2A E3 ligase activity. After purification of the 0.5 M P11 fraction through DEAE5PW and Phenyl Sepharose columns, we determined the relative mass of the enzyme complex on the S300 gel-filtration column and found it to be about 250–

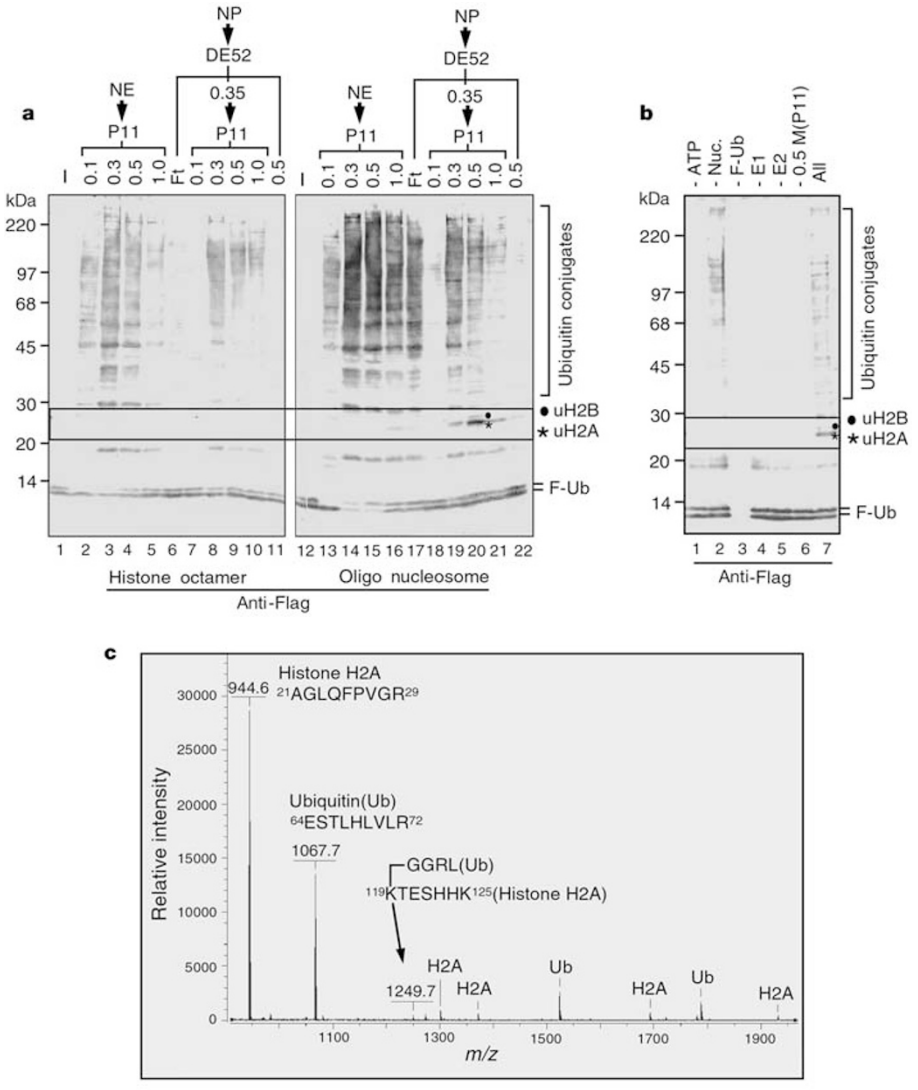

Figure 1 Identification of an H2A ubiquitin ligase activity in HeLa cells. **a**, Ubiquitin ligase assay using HeLa nuclear proteins fractionated on DE52 and P11 columns. Numbers on top of the panels indicate the salt concentration (M) for step elution. NE and NP represent nuclear extracts and nuclear pellet, respectively. Left and right panels use histone octamer and oligonucleosome substrates, respectively. **b**, The ligase activity depends on the presence of ATP, E1, E2, ubiquitin, nucleosomal histones, and proteins present in the 0.5 M P11 nuclear pellet fraction. **c**, Mass spectrometry analysis of the ubiquitinated protein revealed the presence of histone H2A and ubiquitin. A peptide that contains amino acids from both ubiquitin and H2A identifies Lys 119 as the ubiquitination site.

300 kDa (Fig. 2b, top panel). Further purification on two additional columns allowed us to correlate four candidate protein bands (marked by * in Fig. 2c, top panel) with the enzymatic activity (Fig. 2c, second panel). The limited amount of samples prevented further purification of the complex. Thus, we pooled the MonoQ samples between fractions 29–32. After concentration, the samples were resolved using SDS–polyacrylamide gel electrophoresis (SDS–PAGE) and the four candidate protein bands were recovered for identification. Mass spectrometry analysis identified the middle two protein bands as Ring1 and Ring2[10,11], two human homologues of *Drosophila* PRC1 core component dRing/Sce (Sex combs extra)[12–14]. Western blot analysis confirmed that both proteins co-fractionate with the ligase activity on the MonoQ column (Fig. 2c, bottom two panels), as well as on the S300 column

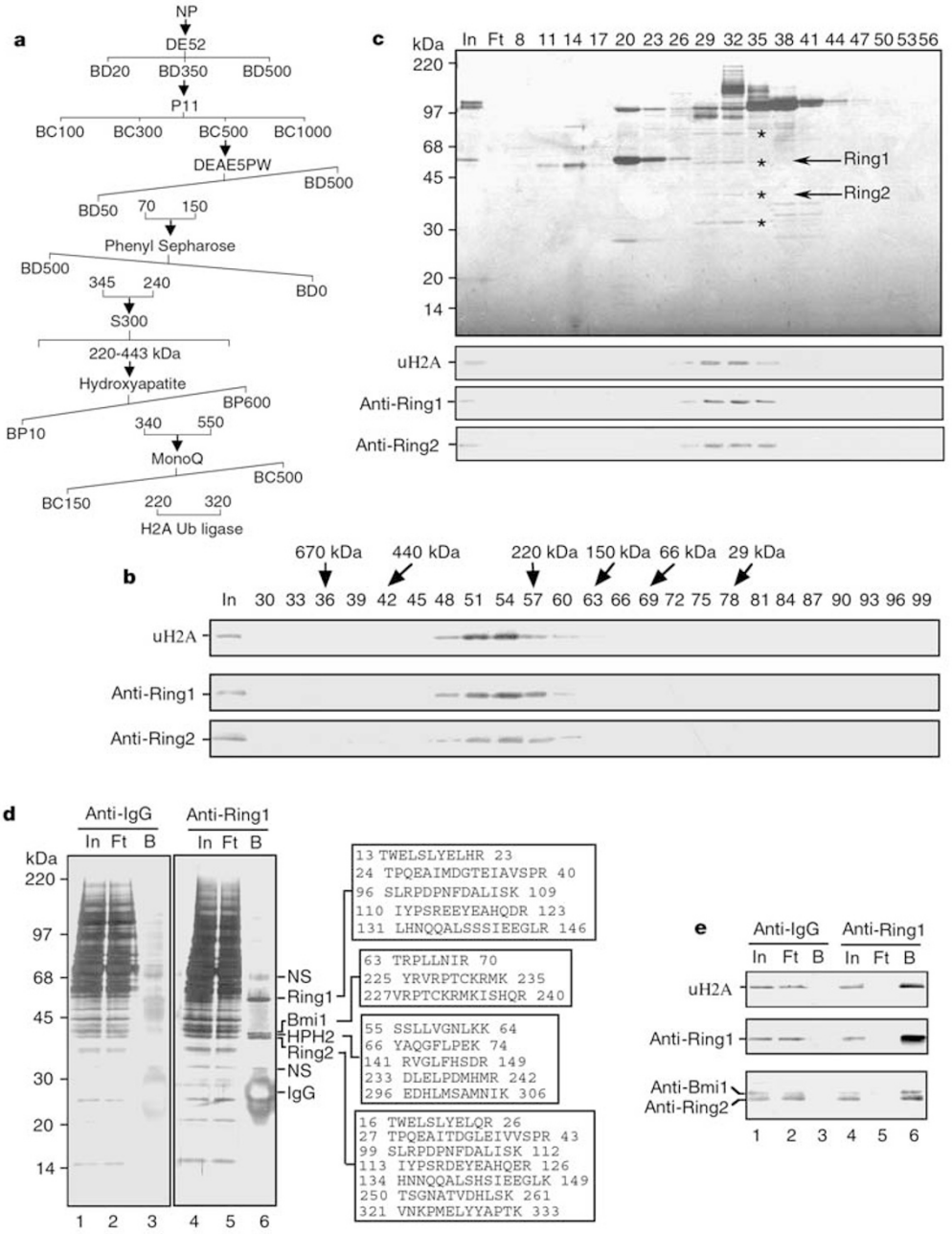

Figure 2 Purification and identification of the H2A ubiquitination ligase complex. **a**, Schematic representation of the steps used to purify the H2A ubiquitination ligase complex. Numbers represent the salt concentrations (mM) at which the E3 ligase activity elutes from the columns. **b**, The H2A ubiquitin ligase activity assay (top panel) and western blot analysis (bottom two panels) of the protein fractions derived from the gel-filtration S300 column. The elution profile of the protein markers is indicated on top of the panel. Antibodies used for the western blot are indicated. **c**, Silver staining of a polyacrylamide–SDS gel (top panel), H2A ubiquitin ligase activity assay (second panel) and western blot analysis (bottom two panels) of the fractions derived from the MonoQ column. The candidate proteins that co-fractionated with the E3 ligase activity are indicated by *. The positions of the protein size markers on SDS–PAGE are indicated to the left of the panel. **d**, Silver staining of polyacrylamide–SDS gels containing samples derived from input (In), flow-through (Ft), and bound (B) using purified rabbit IgG and Ring1 antibodies. The identities of the proteins co-immunoprecipitate with Ring1 are indicated. Peptides derived from each protein band are also indicated. Numbers represent the amino acid number of the respective proteins. NS indicates nonspecific-binding proteins that are also present in the control IP (lane 3). **e**, The same samples presented in **d** were analysed by H2A ubiquitin ligase activity assay (top panel) and western blotting (bottom two panels). Antibodies used are indicated.

(Fig. 2b, bottom two panels). However, we failed to unequivocally identity the other two protein bands.

To define the composition of the E3 ligase complex, we performed immunoaffinity purification using an aliquot of the hydroxyapatite input material and an antibody against Ring1. The affinity-purified samples were split for silver staining, ubiquitin ligase assay, western blotting, and protein identification. Silver staining revealed that anti-Ring1 antibodies specifically immunoprecipitated four protein bands (Fig. 2d, compare lanes 6 and 3). Mass spectrometry analysis identified these proteins as Ring1, Bmi1, HPH2 (human Polyhomeotic 2) and Ring2 (Fig. 2d). The identities of these proteins were also verified by western blotting (Fig. 2e, bottom two panels). The protein complex is apparently responsible for the ligase activity as the activity is depleted in the flow-through (Fig. 2e, top panel, compare lanes 5 and 2). Collectively, the above results allow us to conclude that the H2A ubiquitin E3 ligase complex is composed of four Polycomb group (PcG) proteins including Ring1, Bmi1, HPH2 and Ring2. Given that a human Polycomb repressive complex containing Ring1, Ring2, Bmi1, HPH1, HPH2, HPH3, M33, SNF2H, SCMH1, HSP70 and tubulin has been previously purified from HeLa cell lines expressing Flag-

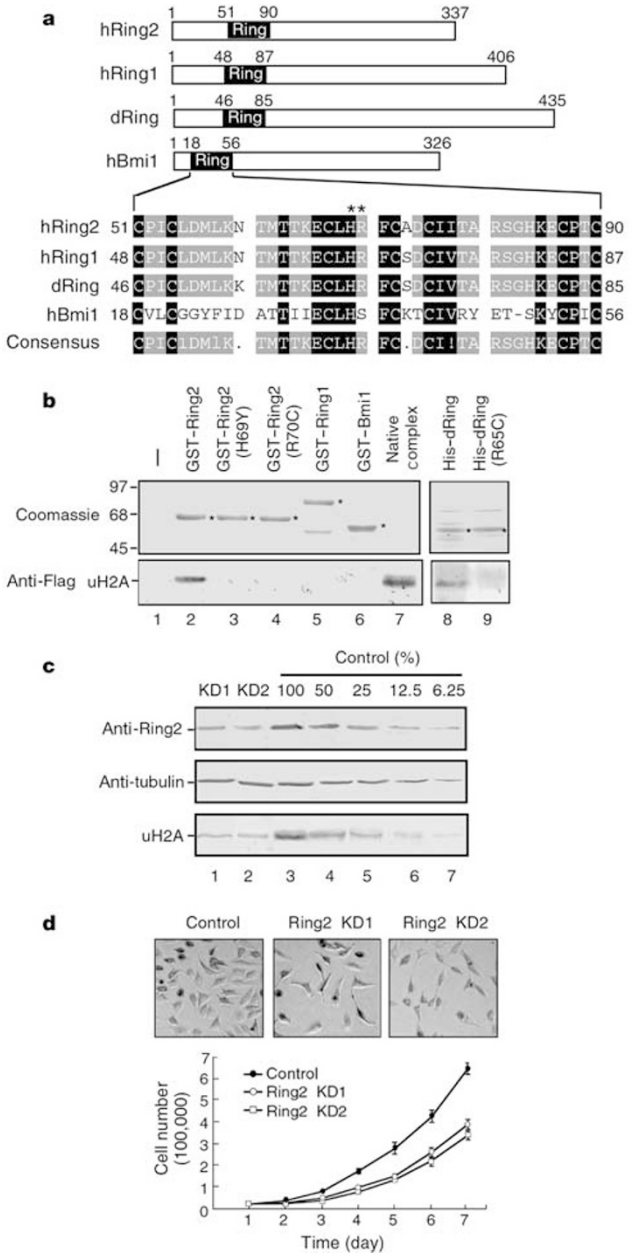

Figure 3 Ring2 is the catalytic subunit and is required for H2A ubiquitination *in vivo*. **a**, Diagram of human Ring1 and Ring2, their *Drosophila* homologue dRing, and human Bim1. A sequence alignment of the RING finger domain of these proteins is shown. Amino acids that are completely conserved are shaded with black. The two Ring2 mutants used in **b** are indicated by *. Numbers represent the amino acid number. **b**, Ubiquitin ligase activity (bottom panel) of recombinant proteins (top panel, lanes 2–6, 8 and 9) and native hPRC1L (lane 7). **c**, Estimation of the Ring2 knock-down level in the KD1 and KD2 cell lines relative to the mock knock-down cells transfected with empty vector. Tubulin was used as a loading control. Antibodies used are indicated on the left of the panel. **d**, Ring2 knock-down results in morphological change and cell growth inhibition. Top panels show morphological changes of control and knock-down HeLa cells. Bottom panel shows the growth curve of control and knock-down HeLa cells. Viable cells were counted by trypan blue staining at different times after initial seeding of 3×10^4 cells.

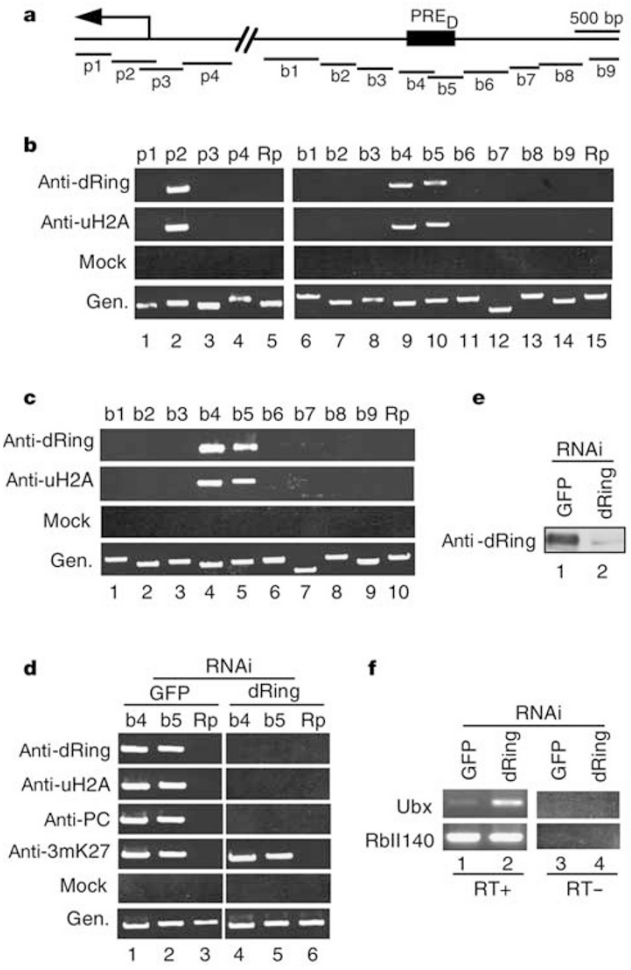

Figure 4 dRing-dependent H2A ubiquitination at *Ubx* PRE and promoter regions. **a**, Schematic representation of the *Ubx* promoter and *bxd* PRE$_D$ regions. The regions amplified by PCR in the ChIP assays are depicted as horizontal lines. **b**, ChIP results showing the wild-type distributions of dRing and ubiquitinated H2A in wing imaginal discs. **c**, ChIP results showing the distribution of dRing, and ubiquitinated H2A at the PRE$_D$ region in normal SL2 cells. **d**, ChIP results of SL2 cells transfected with GFP dsRNA (left panels) or dRing dsRNA (right panels). **b**–**d**, Antibodies used in immunoprecipitations and the PCR amplified regions are indicated to the left and above, respectively. Rp, RpII140 promoter; mock, crude rabbit preimmune-antiserum; Gen, genomic DNA. **e**, Western blots showing dRing levels in SL2 RNAi cells. **f**, dRing knock-down leads to derepression of *Ubx*. Levels of *Ubx* transcripts in cells transfected with GFP or dRing dsRNA was evaluated by RT–PCR. **e** and **f**, SL2 cells transfected twice with GFP or dRing dsRNA. RpII140 expression serves as a control. RT +, reverse transcriptase included in the reaction; RT −, reverse transcriptase omitted.

tagged Bmi1 or M33 and was named hPRC1[15], we have named our complex hPRC1L (human PRC1-like) to reflect the similarity of these two protein complexes.

RING finger has been identified as a signature motif for ubiquitin E3 ligase[16]. Of the four PcG proteins in the H2A ubiquitin E3 ligase complex, three contain RING fingers (Fig. 3a). To determine the catalytic subunit of the E3 ligase complex, we expressed each of the ring-containing proteins as a GST fusion protein (Fig. 3b) and analysed their potential ubiquitin ligase activity using equal amounts of oligonucleosomal substrates. Results shown in Fig. 3b indicate that only recombinant Ring2 is active (bottom panel, compare lanes 2, 5 and 6). To determine whether the RING finger domain of Ring2 is responsible for the enzymatic activity, a conserved His residue involved in zinc binding was mutated to Tyr (H69Y). This change completely abrogated the E3 ligase activity (Fig. 3b, compare lanes 2 and 3), indicating that the RING finger domain of Ring2 is critical for its ubiquitin ligase activity. Previous studies in *Drosophila* have identified a loss of function *dRing/Sce* allele, Sce^{33M2}, that contains a single amino acid substitution (R65C) in the RING finger domain[12]. To analyse the effect of this mutation on the E3 ligase activity, we generated a Ring2 mutant (R70C) that mimics the Sce^{33M2} mutation (Fig. 3a). Interestingly, this mutation also abrogated the Ring2 enzymatic activity (Fig. 3b, compare lanes 2 and 4), raising the possibility that the phenotypes associated with Sce^{33M2} may be linked to defective H2A ubiquitination. To verify this possibility, wild type and a mutant dRing (R65C) that has the same mutation as that of the Sce^{33M2} allele were made and tested for E3 activity. Results shown in Fig. 3b (lanes 8 and 9) demonstrate that wild-type dRing, but not the mutant, has H2A ubiquitin ligase activity. Therefore, we conclude that both Ring2 and dRing contain intrinsic E3 ligase activity and that the conserved Arg 70 (Arg 65 in dRing) in the RING domain is critical for the enzymatic activity.

To investigate the role of Ring2 in H2A ubiquitination *in vivo*, we generated two independent stable Ring2 knock-down cell lines, KD1 and KD2, that target two different regions of human Ring2 messenger RNA for degradation using a vector based short interfering RNA (siRNA) approach[17]. Western blot analysis indicated that about 75% knock-down was achieved at the protein level in both cell lines (Fig. 3c, top panel, compare lanes 1 and 2 with 5). To evaluate the effect of Ring2 knock-down on H2A ubiquitination *in vivo*, we performed western blot analysis using a previously well-characterized[18] uH2A-specific monoclonal antibody E6C5, which can also recognize ubiquitinated H2A from *Drosophila* (Supplementary Fig. S1). Results shown in Fig. 3c indicated a roughly 75% decrease in the uH2A level in the knock-down cells when compared with that of control knock-down cells (bottom panel, compare lanes 1 and 2 with 5). These data strongly suggest that Ring2 is required for H2A ubiquitination *in vivo*. Similar to knock-down of SUZ12[19], an EED-EZH2 HMTase component, Ring2 knock-down resulted in changes in cellular morphology and slower growth (Fig. 3d), consistent with a role of Ring2 in regulating cellular differentiation and proliferation[20].

To understand the functional relationship between dRing-mediated H2A ubiquitination and Hox gene silencing, we focused our study on a well-characterized *Drosophila* PcG target gene, *Ubx*. Silencing of *Ubx* transcription in wing imaginal discs requires both the ESC-E(Z) and PRC1 complexes, in addition to the major PRE (Polycomb response element) within the *bxd* regulatory region (PRE_D) to which the two complexes bind. Having demonstrated the specificity of the E6C5 monoclonal anti-uH2A antibody for *Drosophila* uH2A (Supplementary Fig. S1), we performed chromatin immunoprecipitation (ChIP) assays of wing imaginal disc cells which revealed colocalization of dRing and ubiquitinated H2A at PRE_D and immediately downstream of the *Ubx* transcription start site (Fig. 4b), sites at which E(Z) and PC, another PRC1 core component, have previously been shown to be located[21,22]. Homozygous *Sce*/*dRing* mutants die early in development, precluding ChIP analysis of mutant wing imaginal discs[12]. Therefore, dependence of H2A ubiquitination at PRE_D on dRing was tested using SL2 tissue culture cells.

Previous studies have shown that PC, E(Z) and E(Z)-dependent H3-K27 methylation colocalize at the PRE_D region in SL2 cells[21,22]. As in wing imaginal discs, dRing and ubiquitinated H2A also colocalize at PRE_D (Fig. 4c). Depletion of dRing by RNAi resulted in loss of ubiquitinated H2A, as well as PC from the PRE (Fig. 4d, right panels). E(Z)-dependent trimethylation on H3-K27 was not affected (Fig. 4d, right panels). Loss of dRing, PC and uH2A is accompanied by derepression of *Ubx* gene expression (Fig. 4f), similar to that previously observed upon RNAi-mediated depletion of PC[22]. Because the PRC1 complex appears to be lost along with dRing, we cannot distinguish between the roles of H2A ubiquitination and other potential functions of the PRC1 complex in *Ubx* repression. However, somatic clones that are homozygous for the Sce^{33M2} allele, which contains the R65C substitution within the RING domain, exhibit *Ubx* derepression in wing imaginal discs[12]. Together with the fact that the R65C mutation abolishes dRing ubiquitin ligase activity (Fig. 3b), these observations collectively suggest that dRing-mediated H2A ubiquitination plays an important role in *Ubx* gene silencing.

It is intriguing that ubiquitination of H2A and H2B has opposite effects on transcription. In the case of H2B, ubiquitination is associated with gene activation[23,24], and is required for H3-K4, -K79 methylation, a phenomenon referred to as '*trans*-tail' regulation[7,25,26]. It is yet to be determined whether H2A ubiquitination also participates in *trans*-tail regulation since H3-K27 methylation, a modification that is central to PcG transcriptional silencing, appears to be independent of H2A ubiquitination (Fig. 4d, compare left and right panels). It is possible that H2A ubiquitination may regulate other histone modifications that are associated with PcG-dependent silencing or inhibit modifications required for transcriptional activation. Although the mechanism by which H2A ubiquitination contributes to PcG silencing is currently unknown, identification of the responsible enzyme should allow us to better understand the PcG silencing system. □

Methods

In vitro histone ubiquitin ligase assay and ubiquitination site mapping

Histone octamers (5 μg) or oligonucleosomes (5 μg) were incubated with 20 μl protein fractions or recombinant proteins in a 36 μl reaction containing 50 mM Tris-HCl (pH 7.9), 5 mM $MgCl_2$, 2 mM NaF, 0.6 mM DTT, 2 mM ATP, 10 μM Okada acid, 0.1 μg ubiquitin activating enzyme E1 (Calbiochem), 0.6 μg ubiquitin conjugating enzyme Ubc5c, 1 μg flag-ubiquitin (Sigma). After incubation at 37 °C for 1 h, reaction was terminated by addition of SDS–PAGE loading buffer. The proteins were resolved in 8–15% SDS–PAGE and blotted with the anti-Flag antibody. For ubiquitination site determination, a protein band corresponding to ubiquitinated H2A was excised and subjected to trypsin digestion and MALDI-TOF MS analysis[27]. Identification of a peptide that corresponds to residues 119–125 of H2A (K*TESHHK) linked to (indicated by *) the C-terminal LRGG of ubiquitin suggests that Lys 119 is the site of ubiquitination.

Constructs and antibodies

Plasmids encoding GST–Ring2 and GST–Ring2 (H69Y) were obtained from S. Kang[10]. The GST–Ring2 (R70C) mutant was generated by PCR-based mutagenesis and confirmed by DNA sequencing. Plasmids encoding GST–Ring1 and GST–Bmi1 were constructed by PCR amplification of EST clones (CS0DI076YE14 and CL0BB004ZD04) and the inserts cloned into *Eco*RI and *Xho*I sites of pGEX-KG vector. A plasmid encoding His_6–dRing was constructed by RT–PCR amplification of the RNA from *Drosophila* embryos and the full-length coding sequence inserted into the pQE30 vector. The His_6–dRing (R65C) mutant was generated by replacing a *Pst*I fragment of wild-type dRing with a corresponding fragment from the mutant Sce^{33M2} allele. All the sequences were verified by DNA sequencing. Plasmid for His_6–Ubc5c was a gift from Y. Xiong. Antibodies against uH2A and Bmi1 were purchased from Upstate. Antibodies against PC, H3-3mK27, Ring1 and Ring2 have been previously described[22,28,29]. Antibody against dRing was generated in rabbits by injection of a His_6-dRing fusion protein.

dRing knock-down and ChIP assays

Culture of SL2 cells and transfection with double-stranded RNA, ChIP assays and RT–PCR analysis of *Ubx* transcripts from SL2 cells were performed as previously described[22],

with the exception that ChIP assays were performed on cells harvested 72 h following a single transfection with dsRNA. *dRing* dsRNA including exonic sequences extending from 167 to 1,154 base pairs (bp) downstream of the ATG was synthesized by bi-directional transcription of RT–PCR products containing T7 promoter sequences at both ends. Isolation of wing imaginal discs and ChIP assays were performed as previously described[22].

Information for purification and identification of histone H2A ubiquitin ligase complex, for generation and characterization of Ring2 knock-down cell lines, as well as for the specificity of the uH2A antibody, is available in Supplementary Methods and Supplementary Data.

Received 29 June; accepted 2 September 2004; doi:10.1038/nature02985.

1. Jenuwein, T. & Allis, C. D. Translating the histone code. *Science* **293,** 1074–1080 (2001).
2. Zhang, Y. & Reinberg, D. Transcription regulation by histone methylation: interplay between different covalent modifications of the core histone tails. *Genes Dev.* **15,** 2343–2360 (2001).
3. Zhang, Y. Transcriptional regulation by histone ubiquitination and deubiquitination. *Genes Dev.* **17,** 2733–2740 (2003).
4. Robzyk, K., Recht, J. & Osley, M. A. Rad6-dependent ubiquitination of histone H2B in yeast. *Science* **287,** 501–504 (2000).
5. Hwang, W. W. *et al.* A conserved RING finger protein required for histone H2B monoubiquitination and cell size control. *Mol. Cell* **11,** 261–266 (2003).
6. Wood, A. *et al.* Bre1, an E3 ubiquitin ligase required for recruitment and substrate selection of Rad6 at a promoter. *Mol. Cell* **11,** 267–274 (2003).
7. Sun, Z. W. & Allis, C. D. Ubiquitination of histone H2B regulates H3 methylation and gene silencing in yeast. *Nature* **418,** 104–108 (2002).
8. Dover, J. *et al.* Methylation of histone H3 by COMPASS requires ubiquitination of histone H2B by Rad6. *J. Biol. Chem.* **277,** 28368–28371 (2002).
9. Nickel, B. E. & Davie, J. R. Structure of polyubiquitinated histone H2A. *Biochemistry* **28,** 964–968 (1989).
10. Lee, S. J. *et al.* E3 ligase activity of RING finger proteins that interact with Hip-2, a human ubiquitin-conjugating enzyme. *FEBS Lett.* **503,** 61–64 (2001).
11. Satijn, D. P. *et al.* RING1 is associated with the polycomb group protein complex and acts as a transcriptional repressor. *Mol. Cell. Biol.* **17,** 4105–4113 (1997).
12. Fritsch, C., Beuchle, D. & Muller, J. Molecular and genetic analysis of the Polycomb group gene Sex combs extra/Ring in *Drosophila*. *Mech. Dev.* **120,** 949–954 (2003).
13. Gorfinkiel, N. *et al.* The *Drosophila* Polycomb group gene Sex combs extra encodes the ortholog of mammalian Ring1 proteins. *Mech. Dev.* **121,** 449–462 (2004).
14. Francis, N. J., Saurin, A. J., Shao, Z. & Kingston, R. E. Reconstitution of a functional core polycomb repressive complex. *Mol. Cell* **8,** 545–556 (2001).
15. Levine, S. S. *et al.* The core of the polycomb repressive complex is compositionally and functionally conserved in flies and humans. *Mol. Cell. Biol.* **22,** 6070–6078 (2002).
16. Joazeiro, C. A. & Weissman, A. M. RING finger proteins: mediators of ubiquitin ligase activity. *Cell* **102,** 549–552 (2000).
17. Wang, H. *et al.* mAM facilitates conversion by ESET of dimethyl to trimethyl lysine 9 of histone H3 to cause transcriptional repression. *Mol. Cell* **12,** 475–487 (2003).
18. Vassilev, A. P., Rasmussen, H. H., Christensen, E. I., Nielsen, S. & Celis, J. E. The levels of ubiquitinated histone H2A are highly upregulated in transformed human cells: partial colocalization of uH2A clusters and PCNA/cyclin foci in a fraction of cells in S-phase. *J. Cell Sci.* **108,** 1205–1215 (1995).
19. Cao, R. & Zhang, Y. SUZ12 is required for both the histone methyltransferase activity and the silencing function of the EED-EZH2 complex. *Mol. Cell* **15,** 57–67 (2004).
20. Voncken, J. W. *et al.* Rnf2 (Ring1b) deficiency causes gastrulation arrest and cell cycle inhibition. *Proc. Natl Acad. Sci. USA* **100,** 2468–2473 (2003).
21. Cao, R. *et al.* Role of histone H3 lysine 27 methylation in Polycomb-group silencing. *Science* **298,** 1039–1043 (2002).
22. Wang, L. *et al.* Hierarchical recruitment of polycomb group silencing complexes. *Mol. Cell* **14,** 637–646 (2004).
23. Henry, K. W. *et al.* Transcriptional activation via sequential histone H2B ubiquitylation and deubiquitylation, mediated by SAGA-associated Ubp8. *Genes Dev.* **17,** 2648–2663 (2003).
24. Kao, C. F. *et al.* Rad6 plays a role in transcriptional activation through ubiquitylation of histone H2B. *Genes Dev.* **18,** 184–195 (2004).
25. Ng, H. H., Xu, R. M., Zhang, Y. & Struhl, K. Ubiquitination of histone H2B by Rad6 is required for efficient Dot1-mediated methylation of histone H3 lysine 79. *J. Biol. Chem.* **277,** 34655–34657 (2002).
26. Briggs, S. D. *et al.* Gene silencing: trans-histone regulatory pathway in chromatin. *Nature* **418,** 498 (2002).
27. Devroe, E., Erdjument-Bromage, H., Tempst, P. & Silver, P. A. Human Mob proteins regulate the NDR1 and NDR2 serine-threonine kinases. *J. Biol. Chem.* **279,** 24444–24451 (2004).
28. Plath, K. *et al.* Role of histone H3 lysine 27 methylation in X inactivation. *Science* **300,** 131–135 (2003).
29. Schoorlemmer, J. *et al.* Ring1A is a transcriptional repressor that interacts with the Polycomb-M33 protein and is expressed at rhombomere boundaries in the mouse hindbrain. *EMBO J.* **16,** 5930–5942 (1997).

Supplementary Information accompanies the paper on **www.nature.com/nature**.

Acknowledgements We thank J. Kim for help with mass spectrometry. This work was supported by NIH grants to Y.Z., R.S.J. and P.T.

Competing interests statement The authors declare that they have no competing financial interests.

Correspondence and requests for materials should be addressed to Y.Z. (yi_zhang@med.unc.edu).

corrigenda

The lipid phosphatase SHIP2 controls insulin sensitivity

S. Clément, U. Krause, F. Desmedt, J.-F. Tanti, J. Behrends, X. Pesesse, T. Sasaki, J. Penninger, M. Doherty, W. Malaisse, J. E. Dumont, Y. Le Marchand-Brustel, C. Erneux, L. Hue & S. Schurmans

Nature **409,** 92–96 (2001).

In this Letter, we investigated the production and the phenotypic characterization of a SHIP2 (SH2 domain containing inositol phosphate 5-phosphatase type 2, or *Inppl1*) knockout mice. Total or partial loss of SHIP2 enzyme in these mice resulted in an increased insulin sensitivity. From these experiments, we concluded that SHIP2 is a potent negative regulator of insulin signalling and insulin sensitivity *in vivo*. However, we have recently realized that the 7.3-kilobase genomic DNA fragment deleted in these mice includes, in addition to exons 19–29 of the *SHIP2* gene, the third (and last) exon of the *Phox2a* gene. The deletion of this exon results in the absence of the 124 carboxy-terminal amino acids from a total of 280, including part of the homeodomain, and should give rise to a completely non-functional Phox2a protein if expressed. As a consequence, the mice we described have both *SHIP2* and *Phox2a* genes inactivated. It is currently unknown whether the increased insulin sensitivity we observed in our mice results from the inactivation of the *SHIP2* gene alone, of the *Phox2a* gene alone, or of both genes. □

Induction of DNA methylation and gene silencing by short interfering RNAs in human cells

Hiroaki Kawasaki & Kazunari Taira

Nature **431,** 211–217 (2004).

In the Methods section of this Letter, the published primer sequences used to amplify the E-cadherin and *erbB2* promoters for bisulphite sequencing were incorrect. We used two primer sets, one for unconverted DNAs and the other for converted DNAs. Primers for unconverted DNAs were: for the E-cadherin promoter, the forward primer was 5′-TCTAGAAAAATTTTTTAAAAA-3′ and the reverse primer was 5′-CAGCGCCGAGAGGCTGCGGCT-3′; for the *erbB2* promoter, the forward primer was 5′-CCTGGAAGCCA-CAAGGTAAAC-3′ and reverse primer was 5′-TTTCTCCGG TCCCAATGGAGG-3′. Primers for converted DNAs were: for the E-cadherin promoter, the forward primer was 5′-TTTA-GAAAAATTTTTTAAAAA-3′ and the reverse primer was 5′-CAA-CACCAAAAAACTACAACT-3′; for the *erbB2* promoter, the forward primer was 5′-TTTGGAAGTTATAAGGTAAAT-3′ and the reverse primer was 5′-TTTCTCCAATCCCAATAAAAA-3′. □